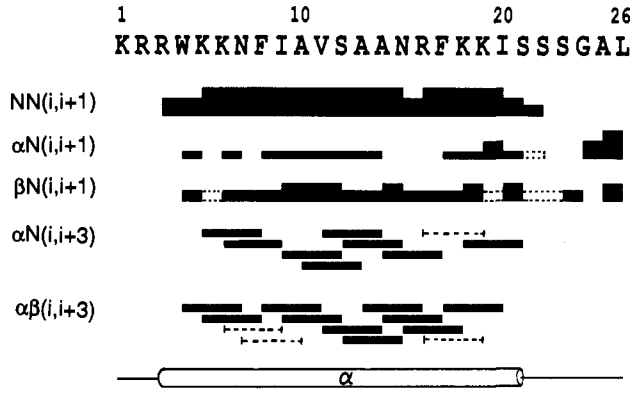

Figure 9. Amino acid sequence of the MLCK peptide (M13) and summary of the short-range NOEs involving HN, CαH, and CβH protons together with the secondary structure deduced from these data. NOEs that are presumably present but which cannot be identified because of resonance overlap are indicated with broken lines.

present study, which indicates that the conformation of the M13 peptide is α-helical when bound to CaM, show that the "central helix" of CaM cannot exist as a single straight helix in its complex with target peptide, because the α-helical peptide is too short to interact with both domains simultaneously. The "central helix" of M13-complexed CaM therefore must bend in order to bring the two globular domains sufficiently close together. The change in molecular shape that accompanies complexation has previously been observed using small angle X-ray scattering.[14-16]

Based on molecular modeling studies, Persechini and Kretsinger[35] reported that the two domains of CaM can easily interact with a helical cylinder-type peptide if one allows only a single kink in the "central helix" by altering the ψ torsion angle of Ser-81. A more recent NMR study[21] indicates a change in the NOE patterns in the "central helix" for residues Lys-75 through Ser-81 upon complexation with M13, suggesting that the disruption of the central helix is more extensive than in the simple Persechini and Kretsinger model. The intermolecular interaction between M13 Ile-9 NH and CaM Tyr-138 Hδ seen in Figure 7 and the NOE between the side chain of M13 Trp-4 and Hα of CaM Phe-99 (Figure 6) suggest that the peptide is aligned in an antiparallel fashion relative to the protein; i.e., the N-terminal end of M13 interacts with the C-terminal domain of CaM. A number of other NOEs, including several between Phe-17 of M13 and Ile-27 of CaM, confirm that the alignment is antiparallel. This orientation of the peptide helix is opposite to that in the model of Persechini and Kretsinger[35] but agrees with the results of cross-linking experiments by O'Neil and DeGrado.[17]

The structure determination of the CaM-M13 complex based on our NMR data is currently in progress and will be reported elsewhere. Whether the MLCK binding site has an α-helical conformation in the intact protein or exists as an unstructured large loop prior to CaM binding is not clear from the present study. To address this question it will be necessary to examine a larger folded domain of the target protein.

The methodology presented here for studying the conformation of a bound ligand is particularly useful when isotopically enriched protein is available, whereas isotopic enrichment of the ligand is prohibitively expensive. Note that even if isotopically labeled ligand could be obtained, isotopic enrichment of the receptor protein generally will be needed anyway to investigate in detail the interaction between ligand and receptor. Therefore, the isotope-filtering experiments described here are generally useful for the study of the ligand in a protein-ligand complex, prior to the study of the ligand-protein interactions.

Acknowledgment. We thank Claude B. Klee for continuous help, encouragement, and stimulating discussions, Marie Krinks for preparing the calmodulin sample used in this study, Frank Delaglio for help with coding the COSY diagonal subtraction routine used in this study, Lewis E. Kay for help with the assignment of the CaM resonances in the CaM-M13 complex, Dennis A. Torchia for many useful suggestions, and Dan Garrett for development of software used in this study. This work was supported by the Intramural AIDS Anti-viral Program of the Office of the Director of the National Institutes of Health.

Registry No. MLCK, 51845-53-5; M13, 99268-57-2.

(35) Persechini, A.; Kretsinger, R. *J. Cardiovas. Pharmacol.* (*S5*) **1988**, *12*, 1-12.

Stable Polarons in Polyacetylene Oligomers: Optical Spectra of Long Polyene Radical Cations

Thomas Bally,*,† Kuno Roth,† W. Tang,† Richard R. Schrock,‡ Konrad Knoll,‡ and Lee Y. Park‡

Contribution from the Institut de Chimie Physique, Université de Fribourg, Pérolles, CH-1700 Fribourg, Switzerland, and Department of Chemistry, Massachusetts Institute of Technology, Cambridge, Massachusetts 02139. *Received September 23, 1991*

Abstract: The radical cations of *tert*-butyl-capped polyenes containing 3-13 conjugated double bonds were generated radiolytically in Freon matrices and investigated by electronic absorption spectroscopy. The observed spectra are in accord with a qualitative MO/CI model which predicts two bands of disparate intensity which both undergo a shift to lower energies as the chain grows longer. Extrapolation to infinite chain length leads to an energy of ~0.4 eV for the second, intense band and ~0.1 eV for the first, weak band. This finding and its implications with regard to the structure of polarons in polyenes and the nature of doped and/or photoexcited polyacetylene are discussed.

1. Introduction

The primary species obtained upon *doping* of polyacetylene $(CH)_x$ are radical cations or radical anions (called polarons P^+/P^- in the language of solid-state physics).[1] The role of these primary species in the conduction mechanism of doped $(CH)_x$ is somewhat elusive because at moderate dopant levels, the concentration of spins is too low to account for the observed conductivities in terms

* To whom correspondence should be addressed.
† University of Fribourg.
‡ Massachusetts Institute of Technology.

(1) Many excellent reviews and monographs have recently been published on the topic of conducting polymers and the theoretical models used to explain their behavior. The presently relevant case of polyacetylene receives special attention in (a) Roth, S.; Bleier, H. *Adv. Phys.* **1987**, *36*, 2385. (b) Heeger, A. J.; Kivelson, S.; Schrieffer, J. R.; Su, W.-P. *Rev. Mod. Phys.* **1988**, *60*, 781. (c) Baeriswyl, D.; Campbell, D. K.; Mazumdar, S. In *The Physics of Conducting Polymer*; Kiss, H., Ed.; Springer: Berlin, 1992.

0002-7863/92/1514-2440$03.00/0

Scheme I. Mechanisms for Photogeneration of Polarons and Solitons in Polyacetylene

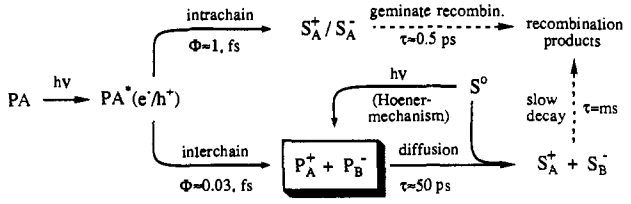

of polarons.[2] It has therefore been proposed that polarons are unstable in doped $(CH)_x$ and collapse to form closed-shell cations and anions (so-called charged solitons S^+/S^-) which are thought to be responsible for the famous "spinless conductivity" of doped $(CH)_x$. These manifest themselves by their "midgap" absorption at ~0.75 eV[3] and by a pair of characteristic IR bands at ~1390 (sharp) and 900 cm^{-1} (broad).[4]

Upon *photoexcitation* of $(CH)_x$ a similar optical signature is found, this time shifted to slightly lower energies (~0.45 eV for the midgap absorption, 540 cm^{-1} for the low-energy IR band)[5] but indicating also the formation of S^+/S^-. There has been much controversy over the last few years over the pathway by which these charged solitons arise following excitation of $(CH)_x$, but it appears today that several mechanisms are effective in contributing simultaneously and/or sequentially to S^+/S^- formation (cf. Scheme I): The incipient electron/hole pair (e^-/h^+) created upon excitation of $(CH)_x$ may separate within femtoseconds into a pair of charged solitons on the same chain (S_A^+/S_A^-) as proposed originally by Su and Schrieffer.[6] Those give rise to a transient 0.45-eV photoinduced absorption (PA) which decays within a few picoseconds after the exciting pulse due to rapid recombination of the soliton pairs.[7,8b]

However, after a delay of ~50 ps a second batch of much more persistent S^+/S^- are formed which are mainly responsible for the photoconductivity of $(CH)_x$ in the millisecond time domain. Following a proposal by Orenstein et al.,[8] these are formed through a process whereby an e^-/h^+ pair is formed on *separate* $(CH)_x$ chains (A/B) which leads to a pair of oppositely charged polarons P_A^+ and P_B^-. These can diffuse along and between chains until they encounter neutral solitons[2] to which they submit their charge,[9] thus creating the charged solitons S_A^+ and S_B^-. The delay is caused by the ~50-meV activation barrier for interchain polaron diffusion in $(CH)_x$.[10] According to a recent proposal by Hoener,[11] P^+/P^- can also be formed by midgap excitation of S° which subsequently abstracts electrons from (or injects electrons into) adjacent $(CH)_x$ chains, thus forming S^+/S^-.

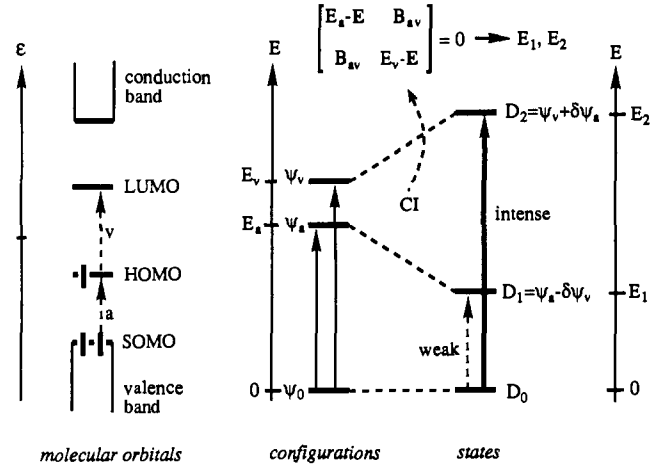

Figure 1. Electronic structure of polyene radical cations: a qualitative MO model (for explanations, see text).

Until 1989 the problem with the above picture was that no direct experimental evidence for the presence of polarons had ever been found. Moreover, theoretical calculations predicted that crystalline three-dimensional $(CH)_x$ lattices are unlikely to support polarons at all,[12] thus fueling skepticism with regard to proposals stipulating polarons in $(CH)_x$. However, two groups recently reported on transient PA's induced by excitation of oriented $(CH)_x$ perpendicular to the chain direction which they attributed to P^+/P^-: Yoshizawa et al. found a 1.4-eV PA decaying with a time constant of 350 ± 40 ns[13] while Rothberg et al. observed a transient 0.35-eV band with a lifetime of "at least 1 ns".[14] It is one of the purposes of this paper to examine if the assignment of these PA's to P^+/P^- in $(CH)_x$ is in accord with extrapolations from oligomers based on the present experimental results.[15]

Our earlier studies on the first few members of linear conjugated polyenes ($(CH)_x$ oligomers) had shown that, under suitable conditions, the corresponding radical cations (polarons) can be stabilized and observed leisurely.[16] Due to the decreasing persistence of the parent polyenes with increasing chain length, these studies could not be extended to $(CH)_x$ oligomers with more than five double bonds. On the other hand, transient spectra of carotenoid radical cations with 9–19 conjugated double bonds were reported some time ago,[18] but a comparison with those of the

(2) In fact, pristine $(CH)_x$ contains ~10^{19} cm^{-3} free spins (neutral solitons S° or odd alternant radicals) which *disappear* during the initial stages of doping, presumably because they are more easily oxidized than closed-shell $(CH)_x$ segments (see Chen, J.; Heeger, A. J. *Synth. Met.* **1988**, *24*, 311 and references cited therein).

(3) (a) Suzuki, N.; Ozaki, M.; Etemad, S.; Heeger, A. J.; MacDiarmid, A. G. *Phys. Rev. Lett.* **1980**, *45*, 1209. (b) Feldblum, A.; Kaufman, J. H.; Etemad, S.; Heeger, A. J.; Chung, T.-C.; MacDiarmid, A. G. *Phys. Rev. B* **1982**, *26*, 815. (c) Chung, T.-C.; Moraes, F.; Flood, J. D.; Heeger, A. J. *Phys. Rev. B* **1984**, *29*, 2341.

(4) Etemad, S.; Pron, A.; Heeger, A. J.; MacDiarmid, A. G.; Mele, E. J.; Rice, M. J. *Phys. Rev. B* **1981**, *23*, 5137.

(5) These shifts can be explained by the absence (presence) of counterions which lead to "pinning" of soliton charges; cf. Schaffer, H.; Friend, R. H.; Heeger, A. J. *Phys. Rev. B* **1987**, *36*, 7537.

(6) Su, W. P.; Schrieffer, J. R. *Proc. Natl. Acad. Sci. U.S.A.* **1980**, *77*, 5626.

(7) Rothberg, T.; Jedju, T. M.; Etemad, S.; Baker, G. L. *Phys. Rev. B* **1987**, *36*, 7529.

(8) (a) Orenstein, J.; Vardeny, Z.; Baker, G. L.; Etemad, S. *Phys. Rev. B* **1984**, *30*, 786. This proposal was recently put into sharp focus by (b) Bleier, H.; Donovan, K.; Friend, R. H.; Roth, S.; Rothberg, L.; Tubino, R.; Vardeny, Z.; Wilson, G. *Synth. Met.* **1989**, *28*, D189.

(9) Odd alternant radicals (alias neutral solitons) are more easily oxidized/reduced than closed-shell polyenes; hence, the P^+/P^- to S° charge transfer is exothermic. An alternative mechanism whereby pairs of charged solitons are formed by recombination of pairs of P^+ or P^- (Moraes, F.; Park, Y. W.; Heeger, A. J. *Synth. Met.* **1986**, *13*, 113) appears unlikely because delayed S^+/S^- formation is largely suppressed in low-spin $(CH)_x$ which contains only few S°.[7]

(10) Walser, A.; Seas, R.; Dorsinville, R.; Alfano, R. R.; Tubino, R. *Solid State Commun.* **1988**, *67*, 333; *Phys. Rev. B* **1991**, *43*, 7194.

(11) Hoener, C. F. *J. Chem. Phys.* **1990**, *92*, 7643.

(12) See for example: Vogl, P.; Campbell, D. K. *Phys. Rev. B* **1990**, *41*, 12797 and references cited therein. Theory predicts that, due to interchain interactions, a single charge injected into crystalline $(CH)_x$ will not induce a localized 1D lattice deformation but will delocalize throughout the bulk material. However, this applies only to a perfectly ordered lattice and may not hold for real-life $(CH)_x$.

(13) (a) Yoshizawa, M.; Kobayashi, T.; Akagi, K.; Shirakawa, H. *Phys. Rev. B* **1988**, *37*, 10301. (b) Yoshizawa, M.; Kobayashi, T.; Fujimoto, H.; Tanaka, J.; Shirakawa, H. *J. Lumin.* **1987**, *38*, 300.

(14) Rothberg, L.; Jedju, T. M.; Townsend, P. D.; Etemad, S.; Baker, G. L. *Mol. Cryst. Liq. Cryst.* **1991**, *194*, 1.

(15) (a) Such extrapolations are often found to be close to linear in $1/n$ (where n is the number of repeating units): Bredas, J. L.; Silbey, R.; Boudreaux, D.; Chance, R. R. *J. Am. Chem. Soc.* **1983**, *105*, 6555. Schaffer, H. E.; Chance, R. R.; Knoll, K.; Schrock, R. R.; Silbey, R. *J. Chem. Phys* **1991**, *94*, 4161. (b) Very recently the first *doped* (conducting) polymer polythiophene, became the target of such an extrapolation: Caspar, J.; Ramamurthy, V.; Corbin, D. R. *J. Am. Chem. Soc.* **1991**, *113*, 594.

(16) (a) Bally, T.; Nitsche, S.; Roth, K.; Haselbach, E. *J. Am. Chem. Soc.* **1984**, *106*, 3927 and references cited therein. (b) Attempts have also been made to stabilize radical cations obtained by $FeCl_3$ or $SbCl_5$ oxidation of polyenes,[17] but this reaction appears to proceed directly to the dications (bipolarons) except for some phenyl-capped derivatives.[17c,d]

(17) (a) Spangler, C. W.; Sapochuk, L. S.; Struck, G. E.; Gates, B. E.; McCoy, R. K. *Polym. Prepr. (Am. Chem. Soc., Div. Polym. Chem.)* **1987**, *28*, 219. (b) Spangler, C. W.; Rathunde, R. A. *J. Chem. Soc., Chem. Commun.* **1989**, 26. (c) Spangler, C. W.; Havelka, K. O. *Polym. Prepr. (Am. Chem. Soc., Div. Polym. Chem.)* **1990**, *31*, 396. (d) Spangler, C. W.; Sapochak, L. S.; Gates, B. D. In *Organic Materials for Non-Linear Optics*; Hahn, R., Bloor, D., Eds. *Spec. Publ.—R. Soc. Chem.* **1989**, *69*, 57.

shorter polyene radical cations ($Pe^{\bullet+}$) indicated that the first, weak transition characteristic of $Pe^{\bullet+}$ (see below) had been missed in the pulse radiolysis experiments.

However, the recent availability of *tert*-butyl-capped polyenes with 3–15 double bonds from controlled oligomerization reactions[19] created the possibility of extending our previous investigations to chain lengths more commensurate with typical conjugation lengths in $(CH)_x$. Also, a comparison of the shorter members of the series with the parent $Pe^{\bullet+}$ would allow us to assess the influence of the terminal alkyl groups and thus draw conclusions with regard to the electronic structure of the longer parent $Pe^{\bullet+}$.

This paper describes the results of this study and the attempts to extrapolate them to infinite chain lengths. After reiterating the qualitative MO/CI model for the electronic structure of $Pe^{\bullet+}$ which served us for the interpretation of the spectra of the shorter members of the series, the newly observed spectra are presented and compared with predictions from this model. Finally the problems encountered in attempts to extrapolate the presently available results to conjugated chains lengths typically found in $(CH)_x$ are discussed.

2. Electronic Structure of Polyene Radical Cations

We have shown in our earlier studies[16a] that the essential features of the electronic structure of $Pe^{\bullet+}$ can be explained on the basis of a simple molecular orbital (MO) model provided that interaction between the first two excited configurations (CI) is taken into account. On the basis of this model (Figure 1) we expect the following trends to emerge as the $Pe^{\bullet+}$ chains grow longer: (a) The energies of the two first excited configurations (E_a and E_v) decrease.[20] (b) Concurrently, the energy gap between E_v and E_a gets smaller. As a consequence, CI between ψ_a and ψ_v becomes more symmetric; i.e., the D_1 and D_2 states approach a 1:1 mixture of ψ_a and ψ_v. (c) On the other hand, the off-diagonal matrix element B_{av} for mixing ψ_a and ψ_v becomes smaller; hence, E_1 and E_2 approach E_a and E_v, respectively.[21] (d) Finally, the electric dipole transition moment vectors for a- and v-excitations become increasingly similar in magnitude and parallel in their orientation, which together with point b above makes their cancellation in D_1 and their addition in D_2 become more efficient.

From the above it follows that for a series of $Pe^{\bullet+}$ with increasing chain length we expect a pair of absorption bands which move closer as their midpoint shifts to lower energies and their intensities become more disparate. Of course we must expect that CI with higher excited configurations of the same symmetry as that of ψ_a and ψ_v will begin to play an increasingly important role as the chains grow longer. This and the effects of geometry relaxation upon ionization (electron–phonon coupling in solid-state physics language), which are not explicitly taken into account, may invalidate the above simple picture for very long chains.

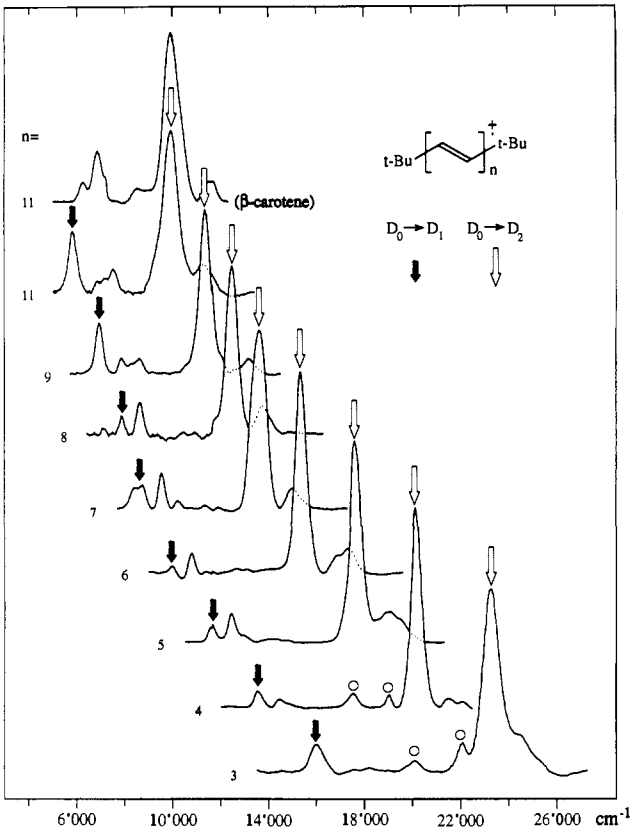

Figure 2. Electronic absorption spectra of *tert*-butyl-capped polyene radical cations with 3–11 double bonds (t-$BuPe_3^{\bullet+}$–t-$BuPe_{11}^{\bullet+}$) obtained in Freon matrices at 77 K. The top spectrum is for β-carotene radical cation (11 conjugated double bonds). Filled arrows point to the first vibronic progression of the $D_0 \rightarrow D_1$ electronic transition (open dots in Figure 4); open arrows indicate the $D_0 \rightarrow D_2$ transition (filled dots in Figure 4). Circles denote bands due to partially cis-configured rotamers which arise in the course of ionization.

Table I. Energies (eV) of the First Two Electronic Transitions in *tert*-Butyl-Capped Polyene Radical Cations (Cf. Spectra in Figure 2)

n	$E(D_0 \rightarrow D_1)^a$	$E(D_0 \rightarrow D_2)$	n	$E(D_0 \rightarrow D_1)^a$	$E(D_0 \rightarrow D_2)$
3	1.98	2.88	8	0.98	1.55
4	1.68	2.49	9	0.86	1.41
5	1.44	2.17	11	0.72	1.23
6	1.24	1.90	11[b]	0.78	1.23
7	1.05	1.69	13	0.63	1.12

[a] First vibronic component (lowest energy peak). [b] β-Carotene.

It is interesting to examine the similarities and differences of the above model to those used to describe the electronic structure of $(CH)_x$ polarons in solid-state physics such as is presented by Fesser et al.:[22] these researchers deduced analytical expressions for the different excitations on the one-electron level ($\psi_0 \rightarrow \psi_a$ and $\psi_0 \rightarrow \psi_v$, left-hand side of Figure 1) but do not consider the possible effects of electron correlation which leads them invariably to the prediction of two absorptions of similar intensity.[23] On the other hand, electron–phonon coupling is taken into account, and we will see that this becomes crucial when we try to extrapolate our results to infinite chain length.

3. Optical Spectra of Polyene Radical Cations

In Figure 2 we present the electronic absorption spectra of the *tert*-butyl-capped polyenes with 3–11 double bonds (t-$BuPe_3$–t-$BuPe_{11}$) as obtained after ~0.5 Mrad γ-irradiation in a Freon mixture (see Experimental Section). The spectrum of β-carotene

(18) (a) Dawe, E. A.; Land, E. J. *J. Chem. Soc., Faraday Trans. 1* **1975**, *71*, 2162. (b) Lafferty, J.; Roach, A.; Sinclair, R. S.; Truscott, T. G.; Land, E. J. *Ibid.* **1977**, *73*, 416. (c) Bensasson, R. V.; Land, E. J.; Truscott, T. G. *Flash Photolysis and Pulse Radiolysis: Contributions to the Chemistry of Biology and Medicine*; Pergamon Press: Oxford, 1983; Chapter 4.

(19) Knoll, K.; Schrock, R. R. *J. Am. Chem. Soc.* **1989**, *111*, 7989.

(20) In Hückel theory, E_a and E_v can be expressed analytically as a function of the chain length n in units of the Hückel resonance integral β for bonded carbon atoms:

$$E_v = 4 \sin\left(\frac{\pi}{2(n+1)}\right)\beta \qquad E_a = E_v \sin\left(\frac{\pi(n-1)}{2(n+1)}\right)\beta$$

Note that these expressions go to zero as n approaches infinity, an artifact which is due to the neglect of bond length alternation at this simple level of theory.

(21) In the zero differential overlap (ZDO) approximation, B_{av} is given by

$$B_{av} = \sum_{i=1}^{n}\sum_{j=1}^{n} c_i^S c_i^H c_j^H c_j^L \gamma_{ij}$$

where the c's are p_z MO coefficients for the highest doubly occupied π-MO (S), the singly occupied π-HOMO (H), and the π-LUMO (L) and γ_{ij} the terms describing the electron repulsion between pairs of electrons in AO's ϕ_i and ϕ_j, respectively. PPP π-SCF calculations using the Mataga–Nishimoto approximation for the electron repulsion integrals were carried out for $Pe^{\bullet+}$ with $2 > n > 50$. A plot of B_{av} vs $1/n$ calculated on this basis extrapolates to $B_{av} = 0$ (T. Bally, unpublished results).

(22) Fesser, K.; Bishop, A. R.; Campbell, D. K. *Phys. Rev. B* **1983**, *27*, 4804.

(23) Note that due to point c above the excited-state *energies* calculated on this level may still be rather accurate.

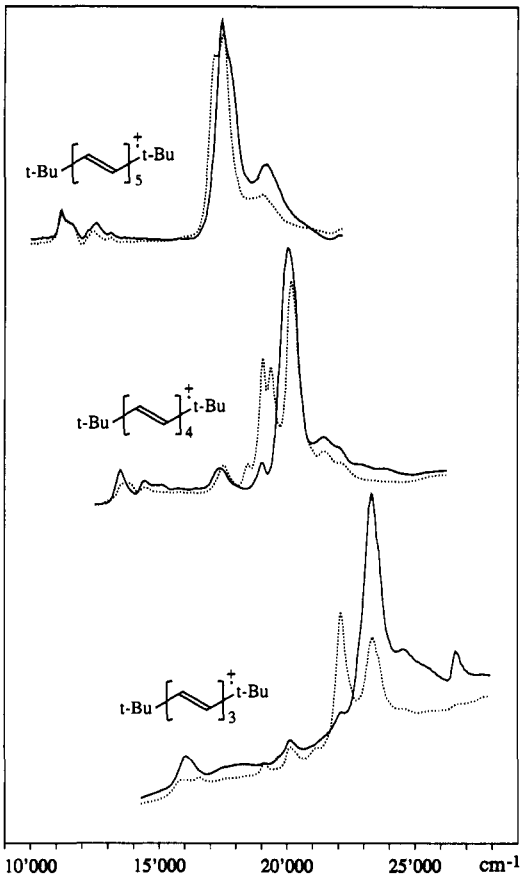

Figure 3. Electronic absorption spectra of *t*-$BuPe_3$–*t*-$BuPe_5$ after ionization (solid lines) and after subsequent photolysis at λ_{max} of the second, intense absorption (broken lines) whereby formation of partially Z-configured rotamers are formed.

(which also has 11 conjugated double bonds) subjected to the same conditions is shown on top for comparison. Unfortunately, we did not succeed in fully separating the *t*-$BuPe_{13}$ compound from *t*-$BuPe_{11}$ and *t*-$BuPe_{15}$, which therefore led to a rather complicated spectrum after ionization. Although we do not show this spectrum in Figure 2, the λ_{max} values for the two excited states of *t*-$BuPe_{13}$ were extracted and used in the extrapolation. The energies of the two electronic transitions are listed in Table I.

It was shown previously that $Pe^{\bullet+}$ exist in the form of several rotamers which can be readily distinguished by the position of their second absorption band; the all-trans rotamer always has the highest energy $D_0 \rightarrow D_2$ transition.[24] The same was found in the *t*-BuPe's, as illustrated in Figure 3, which shows the spectra of *t*-$BuPe_3$ through *t*-$BuPe_5$ immediately after γ-irradiation (solid lines) and after subsequent photolysis at λ_{max} of the second, intense absorption band (dashed lines). Evidently, γ-irradiation results in some rotamerization (the starting materials were single isomers) which can be enhanced further by photolysis, in analogy to what had been observed for the parent polyenes.[24] However, one notes that the spread in $\lambda_{max}(D_0 \rightarrow D_2)$ between the different rotamers decreases as the chains grow longer. By the time one gets to *t*-$BuPe_6$, the spectrum of a mixture of rotamers is only slightly broadened compared to that of the pure all-trans compound. Hence, the fact that the *t*-BuPe's with seven or more double bonds contain alternating cis and trans linkages does not appear to hamper their usefulness in the extrapolation procedure discussed below.

A surprising feature of the spectra in Figure 2 is the shape of the $D_0 \rightarrow D_1$ band which changes in an unusual way along the series; while the 0–0 transition is the most intense one in *t*-$BuPe_3^{\bullet+}$ and *t*-$BuPe_4^{\bullet+}$, it is the second vibronic peak which becomes more prominent in *t*-$BuPe_5^{\bullet+}$–*t*-$BuPe_8^{\bullet+}$, a trend which is, however, again reverted in *t*-$BuPe_9^{\bullet+}$ and *t*-$BuPe_{11}^{\bullet+}$. This phenomenon is indicative of rather abrupt structural changes in the ground and/or the first excited states of the $Pe^{\bullet+}$ as the chains grow longer. We can offer no ready explanation for such changes, but they lead to a problem when it comes to picking the proper peak for the purpose of extrapolation. For the sake of consistency we have therefore always chosen the first rather than the most intense vibronic component of the $D_0 \rightarrow D_1$ transition.

(24) (a) Shida, T.; Kato, T.; Nosaka, Y. *J. Phys. Chem.* **1977**, *81*, 1095. (b) Bally, T.; Nitsche, S.; Roth, K.; Haselbach, E. *Ibid.* **1985**, *89*, 2528. (c) Andrews, L.; Dunkin, I. R.; Kelsall, B. J.; Lurito, J. T. *Ibid.* **1985**, *89*, 821. (d) Bally, T.; Nitsche, S.; Roth, K. *J. Chem. Phys.* **1986**, *84*, 2577.

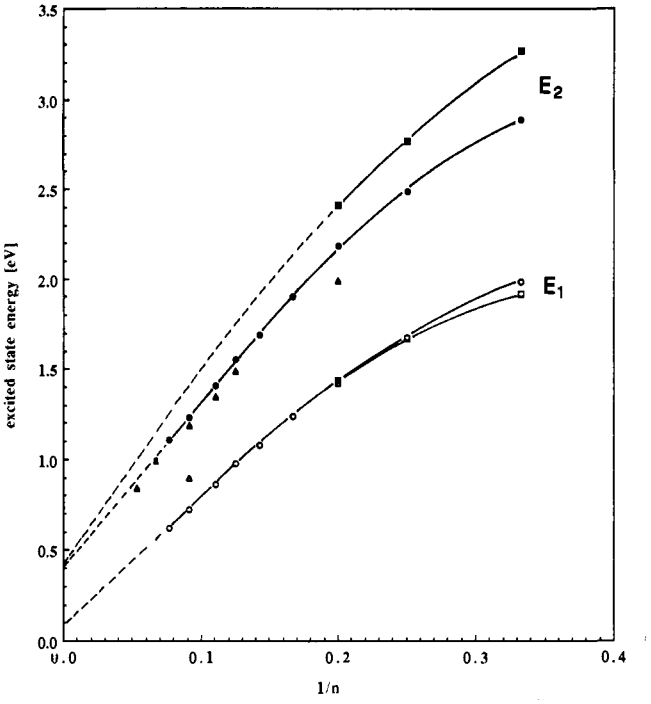

Figure 4. First (E_1, open symbols) and second excited-state energies (E_2, filled symbols) of polyene radical cations as a function of the number of double bonds (n). Squares are for parent $Pe^{\bullet+}$ (n = 3–5), circles for *tert*-butyl-capped $Pe^{\bullet+}$ (n = 3–13), and triangles for retinol radical cation (n = 5) and for carotenoid $Pe^{\bullet+}$ (n = 9, 11, 13, 15, 19).

If we look at the spectra in light of the discussion in section 2, we find that they follow the anticipated trends rather well: as the chains get longer, the two absorption bands move closer while their midpoint shifts to lower energies. The only predicted feature which is not borne out clearly by the *t*-$BuPe^{\bullet+}$ spectra is the increasing disparity in intensity between the first and the second absorption bands as it had been found for the first four members of the unsubstituted all-trans $P^{\bullet+}$.[16a,24c] One reason for this might be that, for *t*-BuPe with seven or more double bonds, the dominant rotamers are partially cis-configured ones. There, the $\psi_0 \rightarrow \psi_a$ and the $\psi_0 \rightarrow \psi_v$ transition dipoles are not as well aligned as in the all-trans rotamers, and hence the disparity in magnitude of their vector addition and subtraction products is less pronounced. Also, it may be that for long chains CI with higher excited configurations reverses the trend which was observed so clearly for the parent compounds with 2–5 double bonds.

In conclusion of this section we can say that, upon removal of an electron, *t*-BuP's with up to 13 double bonds exhibit optical spectra which are typical for linear conjugated polyene radical cations which have their charge and spin essentially delocalized along the entire length of the chain. The same is true for β-carotene and the longer carotenoid polyenes investigated previously. In particular, the present experiments give no indication of a qualitative change in the nature of the electronic and molecular structure of $Pe^{\bullet+}$ upon extending the chain length.

4. Extrapolation to Longer Chains

In Figure 4 we have assembled all the presently known data on the electronic structure of $Pe^{\bullet+}$ in a plot of the first two excited-state energies vs the inverse of the number of double bonds

$(1/n)$. The filled and the open symbols represent data from unsubstituted (squares)[16a,24c] and *tert*-butyl-capped polyenes (circles), respectively, while the filled triangles represent retinoid[25] and carotenoid polyenes[18] investigated earlier by pulse radiolysis. The D_2 energies of the latter are very close to those of the corresponding *t*-BuPe$^{\bullet+}$, but apparently the first transitions had been missed in the above experiments, so the only D_1 energy of such a compound is for β-carotene from the present study (cf. Figure 2, top spectrum).

To the extent that substituted and parent Pe$^{\bullet+}$ can be compared, we find that the shift induced by *tert*-butyl substitution is more pronounced in D_2 than in D_1. In both cases the effect diminishes as the chain length increases, which is to be expected, since for infinitely long Pe$^{\bullet+}$, the presence or absence of terminal *tert*-butyl groups should no longer have a discernible effect; i.e., the two curves should meet as $1/n$ goes to zero, as indicated in Figure 4 (broken line). As in the case of the neutral optical spectra[15a,26] the E vs $1/n$ plot appears to become linear for $n \geq 5$. Extrapolation of these lines to infinity leads to intercepts of ~0.4 eV (3200 cm^{-1}) for D_2 and ~0.1 eV (800 cm^{-1}) for D_1.

However, it can be reasoned that in the present case a linear extrapolation is not valid because theoretical evidence indicates that the spin and charge which determine the electronic structure of Pe$^{\bullet+}$ tend to accumulate in a region with weak bond length alternation around the center of the molecule (cf. following section). In short Pe$^{\bullet+}$ this region encompasses the entire molecule, but for longer chains the extent of spin and charge delocalization will gradually become independent of the extent of conjugation, and therefore the E vs $1/n$ plot is expected to level off at some point and meet the abscissa horizontally. It is the purpose of the following section to examine at which point this flattening will set in and how it will affect the energies of the two Pe$^{\bullet+}$ excited states.

5. Structure of Polarons in Pe$^{\bullet+}$

Following the "discovery" of the polaron in molecular dynamics calculations on $(CH)_x$,[6] predictions of the structure of this novel entity based on the different theoretical models began to appear.[27] In the continuum limit, analytical solutions for the "order parameter" (the difference Δr between the lengths of adjacent C–C bonds in $(CH)_x$) were derived and it was shown that the Δr pattern showed a "dip" or "bag" around the center of the molecule,[27b] which indicated a region of attenuated bond length alternation surrounded by peripheral regions with a geometry similar to that of neutral polyenes.[28]

In our earlier PPP–CI calculations of Pe$^{\bullet+}$ excited states,[16a] we had assumed $\Delta r = 0$ throughout the chains, a simplification which appeared reasonable in view of the small alternation in Hückel π bond orders for short Pe$^{\bullet+}$, and in fact did not prevent the model from reproducing the qualitative trends in E_1 and E_2 correctly. We thought that an extension of these calculations to longer chains would lead to an estimate for the number of double bonds needed to induce the expected flattening of the E vs $1/n$ curves. However, it was evident that now accurate Pe$^{\bullet+}$ geometries were needed to model this correctly.

Previous work by Boudreaux et al.[29] had indicated that the semiempirical MNDO model[30] appears to be well suited for our present purpose in that the Δr pattern calculated for Pe$^{\bullet+}$ was

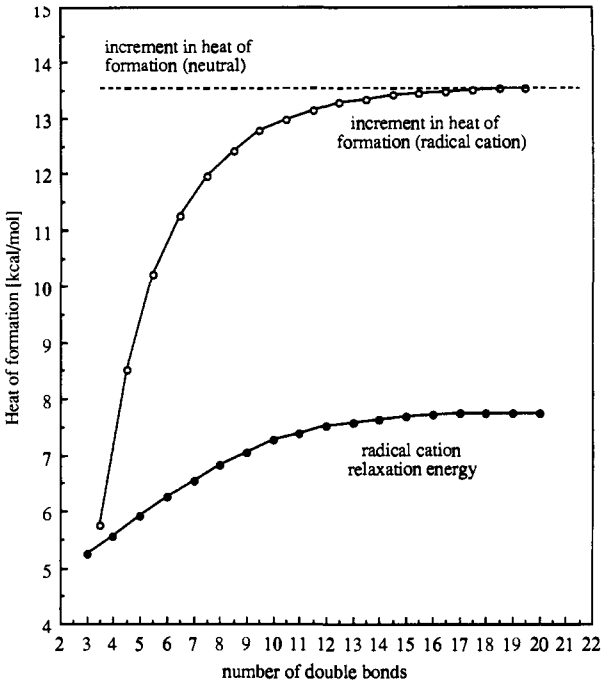

Figure 5. Thermochemical data for Pe$^{\bullet+}$ with 3–20 double bonds as calculated by MNDO/AUHF. The upper line (open dots) shows $\Delta(\Delta H_f°)$ for each additional double bond while the lower line (solid dots) shows the difference between vertical and adiabatic ionization energies of the neutral polyenes.

in good accord with continuum-model predictions. For a realistic modeling of the spin distribution, we preferred to use the UHF variant of MNDO, but in order to avoid problems due to heavy mixing between spin states in the case of Pe$^{\bullet+}$ [31] we employed a version of MNDO/UHF where all higher spin components (quartets, sextets) are annihilated after every SCF iteration.[32] The geometries of all Pe$^{\bullet+}$ were fully optimized within the C_{2h} point group.[35]

Some pertinent results of this exercise, which covered Pe$^{\bullet+}$ with 3–21 double bonds,[35] are presented in Figures 5 and 6. These show that an extension of the Pe$^{\bullet+}$ chain beyond about 15 double bonds hardly affects the delocalization of spin and charge, i.e., the size of the defect which is responsible for the electronic structure of Pe$^{\bullet+}$. This expresses itself for example in the fact that the energy gained by relaxing the Pe$^{\bullet+}$ from the geometry of the corresponding neutral polyene (the vertical minus adiabatic ionization energy, filled dots) becomes nearly constant for Pe$^{\bullet+}$ with more than 15 double bonds. The same is true for the $\Delta H_f°$

(25) The value for $n = 5$ is for retinol (Bobrowski, K.; Das, P. K. *J. Phys. Chem.* **1985**, *8*, 5079).

(26) Kohler, B. E.; Spangler, C.; Westerfield, C. *J. Chem. Phys.* **1988**, *89*, 5422.

(27) (a) Campbell, D. K.; Bishop, A. R. *Phys. Rev. B* **1981**, *24*, 4859; (b) Campbell, D. K.; Bishop, A. R. *Nucl. Phys. B* **1982**, *200*, 297; (c) Brazovskii, S. A.; Kirova, N. *Pisma Zh. Eksp. Teor. Fiz.* **1981**, *33*, 6.

(28) The simplest form for the analytical expression is $\Delta r = \Delta r_\infty[(1-\alpha)\,\mathrm{sech}^2(N/l)]$ where Δr_∞ is Δr for neutral polyenes, N is the number of carbon atoms relative to the center of the molecule, α is a measure for the depth, and l represents the half-width of the dip or bag (from ref 39). Different models or parameter sets yielded predictions for the half-width l of the Δr dip, i.e., the "extent" of polarons in $(CH)_x$ which range between 7 and 10 carbon atoms.

(29) Boudreaux, D. S.; Chance, R. R.; Brédas, J. L.; Silbey, R. *Phys. Rev. B* **1983**, *28*, 258.

(30) Dewar, M. J. S.; Thiel, W. *J. Am. Chem. Soc.* **1977**, *99*, 4899, 4907.

(31) It has been recognized previously that UHF schemes favor Pe$^{\bullet+}$ geometries with nonalternating bond lengths (Kertesz, M. *Adv. Quantum Chem.* **1982**, *15*, 161). We believe that this is at least in part due to mixing with higher spin states which is very pronounced in this case: for a C_{24}Pe$^{\bullet+}$, the expectation value of the S^2 operator is 4.12, i.e., closer to that for a quartet (7.5) than that for a doublet (0.75)!

(32) This so-called AUHF procedure[33] has been implemented in the VAMP program package[34] because it generally presents some advantages in geometry optimizations over the "$^1/_2$-electron" RHF method while giving very similar results. In all Pe$^{\bullet+}$ the final UHF wave functions were of nearly pure doublet character ($\langle S^2\rangle \approx 0.75$). Note that this does not affect spin polarization which leads to the negative spin densities typical of odd alternant polyenyl radicals.

(33) Kovar, T.; Clark, T. Manuscript in preparation.

(34) Vectorized version of AMPAC: Clark, T. Unpublished results. Program for Convex computers available from Professor Clark upon request.

(35) We also attempted to find stationary points corresponding to geometries where spin and charge are localized in opposite halves of the Pe$^{\bullet+}$ (neutral and charged soliton situated on separate kinks). Thus, a C_{22} Pe$^{\bullet+}$ was constructed by joining a separately optimized C_{11} closed-shell cation (S^+) and a C_{11} radical ($S°$) via a 1.46-Å C–C bond. The resulting species showed minimal "leakage" of spin and charge into the "opposite" half of the Pe$^{\bullet+}$; i.e., it conformed to a localized soliton picture.[36] However, upon full geometry optimization it relaxed to C_{2h} symmetry (which was not imposed in this case) and thereby dropped by 6.8 kcal/mol in energy.

(36) Full details (geometries, charge, and spin distributions, etc.) are available from T.B. on request.

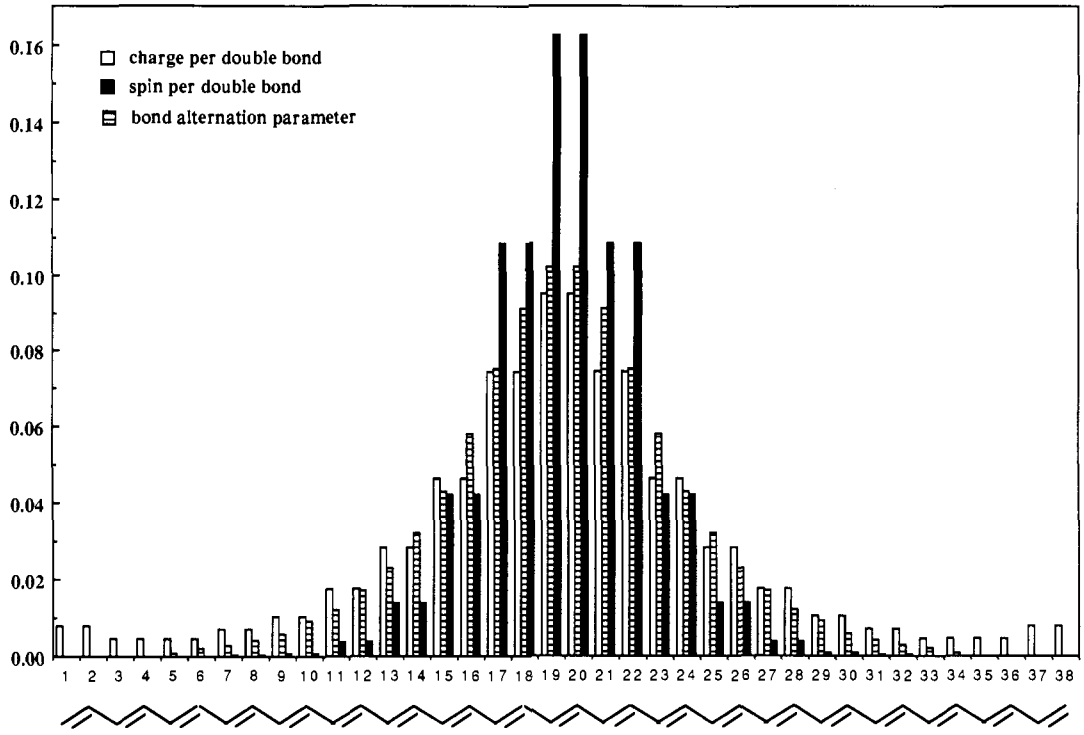

Figure 6. Charge (open bars) and spin (solid bars) per double bond on a C_{38} $Pe^{\bullet+}$ (the corresponding values per carbon atom show oscillations and are averaged for clarity of presentation). The hashed bars show the differences between Pe and $Pe^{\bullet+}$ of the parameter $u_i = (\Delta r)(-1)^i$ where Δr is the difference in adjacent bond lengths. The size of this quantity is indicative of the difference in geometry between Pe and $Pe^{\bullet+}$ at any center in the chain. All values are from MNDO/AUHF calculations.

increment per $-(CH{=}CH)-$ unit (open dots) which approaches that for neutral Pe (13.54 kcal/mol in MNDO) in the same region.

Alternatively, Figure 6 illustrates the extent of spin and charge delocalization in a C_{38} $Pe^{\bullet+}$: while >99.9% of the spin resides within the central 15 double bonds, about 6% of the charge spreads outside this region. However, the bond alternation parameter indicates that this does not affect the geometry, which is almost indistinguishable from that of the corresponding neutral polyene in the three terminal double bonds on both ends, in agreement with the above-mentioned Δr predictions from continuum theories.[27]

On the basis of the MNDO-optimized $Pe_2^{\bullet+}$–$Pe_{40}^{\bullet+}$ geometries, we performed open-shell PPP–CI calculations.[37] Unfortunately, these gave rather bizarre results (to be discussed in more detail in a separate publication[38]) and were of no use for the present purpose. Nevertheless, the MNDO results tell us is that the *ground-state* electronic structure of $Pe^{\bullet+}$ changes only minimally beyond about 15 double bonds. Whether this is also the case for *excited states* is another matter. Intuitively one would assume that upon electronic excitation spin and charge tend to spread out more, i.e., that $Pe^{\bullet+}$ excited states continue to gain stabilization through chain extension beyond the region where the ground-state electronic structure becomes invariant. This would explain why the experimental E vs $1/n$ curves show no tendency to deviate from linearity up to 19 double bonds.

However, a recent MNDO calculation which addressed similar questions for polyynes (which contain $-C{\equiv}C-$ instead of $-CH{=}CH-$ units) came to the conclusion that the structural defect and the spin density wave become *more localized* upon electronic excitation.[39] In spite of the fact that the electronic structures of polyene and polyyne radical ions cannot be directly compared,[40] this result is rather surprising. We plan to apply the methodology used by Williams[39] to the present case of $Pe^{\bullet+}$.

Thus, the question remains whether our results can provide a reasonable estimate of the excited-state energies of a polaron in an infinitely long $Pe^{\bullet+}$. All we can say at present is that E_2 (which is associated with an intense transition) must lie somewhere between ~0.4 eV (the value obtained by linear extrapolation) and 0.83 eV (the energy of the second band in the longest $Pe^{\bullet+}$ observed so far) while the first excited state should give rise to an additional, weaker electronic transition in the IR region. It is to be hoped that in the future suitable theoretical models will be able to produce reliable predictions of E_1 and E_2 as well as the oscillator strengths for the two electronic transitions.

6. The Electronic Structure of Polarons in Polyacetylene

As mentioned in the Introduction, one of the purposes of the present investigation was to examine whether the above conclusions have any bearing on the identification of polarons in $(CH)_x$.[13,14] An important point to note in this context is that in our experiments we deal with *isolated* $Pe^{\bullet+}$ (surrounded by the inert Freon solvent) whereas in $(CH)_x$ strong interchain interactions are likely to prevail. It is a well-known fact that planar π-radical cations have a strong tendency to form sandwich-type complexes with the corresponding neutrals where spin and charge are delocalized over several molecules.[41a] In addition to the local excitations which are often slightly shifted, these complex cations show broad near-IR bands (typically between 0.7 and 1.4 eV), which are

(37) (a) Zahradnik, R.; Carsky, P. *J. Phys. Chem.* **1970**, *74*, 1235. (b) In order for the bond alternation to express itself palpably in this model, it is necessary to scale the resonance integrals β by the deviation of the bond lengths from an average value. In our calculations we used the expression $\beta = \beta_0 - k(r_0 - r)$ where $\beta_0 = -2.318$ eV and $r_0 = 1.4096$ Å (the MNDO-calculated C–C bond length at the center of long $Pe^{\bullet+}$ where $\Delta r = 0$). $k = 2$ was found to give the best results for short $Pe^{\bullet+}$.

(38) T. Bally, to be published. In sum, PPP–CI reproduced E_1 and E_2 in a qualitatively correct fashion up to $n = 10$ whereupon the two first excited configurations began to *diverge* in energy. For $n > 20$ E_1 actually *increased* again, and it appeared as though E_2 would also increase for $n > 50$! We believe that this strange behavior can be traced back to an artifact of the "half-electron" method by which open-shell species are treated in the Longuet-Higgins/Pople SCF algorithm employed in the PPP method. The β-scaling procedure[37b] did nothing to alleviate this problem but instead led to an even earlier divergence of E_1 and E_2. Hence, the PPP–CI procedure which has proven invaluable for electronic structure calculations of many planar π-radical ions appears to be unsuitable in the present case.

(39) Williams, G. R. J. *Synth. Met.* **1989**, *31*, 61.

(40) Bally, T.; Tang, W.; Jungen, M. *Chem. Phys. Lett.* **1992**, *190*, 453.

(41) (a) Badger, B.; Brocklehurst, B. *Trans. Faraday Soc.* **1969**, *65*, 2576, 2582, 2588. (b) Badger, B.; Brocklehurst, B. *Trans. Faraday Soc.* **1970**. *66*, 2989.

attributed to so-called "charge resonance" excitations.[41b] Due to their inherent broadness, these transitions would probably be difficult to detect in $(CH)_x$ polarons, but the above-mentioned shifts induced in the local absorptions through interactions with neighboring $(CH)_x$ chains may constitute a factor which could thwart efforts to extrapolate oligomer data to the case of P^+/P^- in $(CH)_x$.

With the above caveat in mind, we can nevertheless say that our findings are not in contradiction with the assignment of a ~0.35-eV transient PA in $(CH)_x$ to polarons[14] (in fact, linear extrapolation of the oligomer E_2 energies leads very close to this energy). On the other hand, a 1.4-eV absorption[13] is difficult to reconcile with our results which indicate that the intense second transition (which is probably the only one which can be detected in transient PA experiments) should lie well below 1 eV, perhaps even below 0.5 eV, even if it is slightly shifted from the local transition in isolated $Pe^{\bullet+}$. Our findings therefore call for a reinterpretation of the results obtained by Yoshizawa et al.[13]

7. Summary

We have obtained electronic absorption spectra of polyene radical cations ($Pe^{\bullet+}$) with 3-13 conjugated double bonds capped by *tert*-butyl groups. These spectra are discussed within the framework of a simple MO/CI model which correctly predicts the occurrence of an intense high-energy and a weak low-energy electronic transition. Transient absorption spectra of carotenoid $Pe^{\bullet+}$ with 11-19 double bonds obtained previously by pulse radiolysis fit in very well with the present set of data except that a low-energy transition in these compounds had been missed in the earlier studies.

A linear extrapolation of E_1 and E_2 vs $1/n$ plots to infinite chain lengths leads to intercepts of ~0.4 eV (3200 cm^{-1}) for the intense second and ~0.1 eV (800 cm^{-1}) for the weak first electronic transition. The first of these values is in good agreement with the energy of a new band which was recently detected after photoexcitation of oriented all-trans polyacetylene[14] which suggests that an interpretation of this excitation in terms of polarons may be correct. In contrast, the assignment of a transient photoinduced absorption at 1.4 eV to polarons[13] appears questionable in view of the present results, in spite of the fact that the two experiments cannot be directly compared due to the presence of interchain interactions in polyacetlyene.

MNDO calculations show that the ground-state electronic structure of $Pe^{\bullet+}$ (delocalization of spin and charge) changes only minimally as the chain length increases beyond ~0.5 double bonds which indicates that a linear extrapolation may not be valid in this case. In spite of this, the experimental $E_{1,2}$ vs $1/n$ plots show no deviation from linearity up to 19 double bonds which may be taken as evidence that spin and charge are less confined in $Pe^{\bullet+}$ excited states, in contrast to predictions from recent calculations.

8. Experimental Section

The *tert*-butyl-capped polyenes were synthesized at MIT according to the procedures outlined in ref 19. Since the samples with uneven numbers of double bonds were always mixtures of different rotamers, they were subjected to semipreparative HPLC on an analytical reversed-phase column prior to the spectroscopic measurements (C18 by Macherey Nagel, $CH_3CN(80)/H_2O(10)/CH_2Cl_2(5-10)$, 0.5-1 mL/min). In this way, the polyenes were rigorously purified and single rotamers could be significantly enriched in small but sufficient amounts.

The polyenes were dissolved to a concentration of $(2-5) \times 10^{-4}$ M in a 1:1 mixture of two Freons (CF_3Cl and CF_2Br-CF_2Br) and frozen to 77 K. After a reference spectrum was taken, the samples were exposed to ~0.5 Mrad of ^{60}Co γ-radiation whereupon the difference spectra (after minus before ionization) depicted in Figures 2 and 3 were obtained. For t-$BuPe^{\bullet+}$ with $n \leq 5$ it was possible to induce rotamerization by monochromatic photolysis as it had been observed before for the parent $Pe^{\bullet+}$. On the basis of this previous experience, we can say that in these cases the incipient $Pe^{\bullet+}$ was always the all-trans rotamer because it had the lowest $\lambda_{max}(D_2)$.

MNDO calculations were done with the VAMP program package[34] on a CONVEX C120 minisupercomputer.

Acknowledgment. This work is part of Project No. 20-28842.90 of the Swiss National Science Foundation, and at MIT was supported by the Office of Basic Energy Research, Office of Basic Energy Sciences, Chemical Sciences Division of the U. S. Department of Energy (Contract DE-FG02-86ER13564). We thank our colleagues D. Baeriswyl (University of Fribourg), J. Frommer (IBM Almaden), R. Silbey (MIT), and B. Kohler (University of California, Riverside) for invaluable advice and comments and Prof. E. Haselbach for continuing support and encouragement.

η_2 versus η_1 Coordination of Aldehydes and Ketones in Organometallic Complexes. A Semiempirical Theoretical Study

Françoise Delbecq* and Philippe Sautet

Contribution from the Institut de Recherche sur la Catalyse, 2 avenue Einstein, 69626 Villeurbanne Cedex, France, and Ecole Normale Supérieure de Lyon, 46 allée d'Italie, 69364 Lyon Cedex 07, France. *Received February 28, 1991*

Abstract: The η_1 and η_2 coordinations of aldehydes and ketones on several types of organometallic fragments have been compared on the basis of an extended Hückel molecular orbital analysis. The electronic description of the interaction between the organic ligand and the metallic part leads to the distinction between stabilizing two electron interactions and destabilizing four electron ones. The stabilizing interactions concern the frontier orbitals, oxygen lone pair with the LUMO of the metallic fragment for the η_1 mode, and π^*_{CO} with occupied d for the η_2 mode and always favor the η_2 coordination. However, four electron interactions between low-lying orbitals play an important role in the determination of the preferred structure. These interactions result from an indirect coupling through the metal center between occupied orbitals of the organic molecule and those of other ligands on the complex. For overlap reasons these ligand-ligand "through-bond" interactions are stronger for the η_2 mode, thus making this structure less energetically favored. The balance between these two conflicting electronic effects is described for various metals, ligand environments, and substituents on the organic molecule. On this basis, the behavior of d^{10} ML_2, d^8 ML_3, d^6 ML_5, and $CpML_2$ type fragments is detailed. We show how the preferred coordination can be changed for a given type of organometallic fragment by a modification of ligands or substituents.

I. Introduction

Over the past decade, there have been numerous experimental results regarding organometallic complexes having aldehydes and ketones as ligands. Most of them have been isolated and characterized by X-ray spectroscopy, while the others have been analyzed only by IR spectroscopy (for a review see footnote 1 and

0002-7863/92/1514-2446$03.00/0